

3-D Hydrogen-Bonded Frameworks of Two Metal Complexes with Chelidamic Acid: Syntheses, Structures and Magnetism

Guo-Wei Zhou,^{*,‡} Guo-Cong Guo,^{*,‡} Bing Liu,^{*,‡} Ming-Sheng Wang,^{†,‡} Li-Zhen Cai,[†] and Jin-Shun Huang[†]

[†]State Key Laboratory of Structural Chemistry, Fujian Institute of Research on the Structure of Matter, Chinese Academy of Sciences, Fuzhou, Fujian 350002, P. R. China

[‡]Graduate School of Chinese Academy of Sciences, Beijing 100039, P. R. China

Received February 13, 2004

Complexes $M(\text{C}_7\text{H}_2\text{NO}_5)_3\text{H}_2\text{O}\cdot\text{H}_2\text{O}\cdot 0.25\text{MeCN}$ ($M=\text{Ni}, \text{Co}$) were crystallized from the reactions of $\text{Ni}(\text{CH}_3\text{COO})_2\cdot 4\text{H}_2\text{O}$ or $\text{Co}(\text{CH}_3\text{COO})_2\cdot 2\text{H}_2\text{O}$ with KSCN and 2,6-dicarboxy-4-hydroxypyridine (chelidamic acid). The structures were characterized by X-ray crystallography. The crystal structures of **1** and **2** show a distorted octahedral coordination geometry around the M(II) ions, which are chelated by one nitrogen atom and two oxygen atoms of the chelidamic acid and three water molecules. Complexes **1** and **2** display the hydrogen-bonded 3D framework. The magnetic behavior of **2** exhibits antiferromagnetic interaction.

Key Words : Crystal structures, Chelidamic acid, Antiferromagnetic interaction

Introduction

Chelidamic acid (H_3Chel) is used widely in biochemistry, organic chemistry, medical chemistry and even in HIV investigation.¹⁻⁷ In addition, as an emblematical polydentate ligand, it was also of great interest in the study of coordination chemistry. Though the initial report of H_3Chel was published in 1926,⁸ the crystal structure of the H_3Chel was not determined until 2000.⁹ In contrast, the studies concerning the transition metal complexes with chelidamic acid are rare. To our best knowledge, the only known examples consisting of Cr, Fe, Sn, Gd, V and Zn up to now.¹⁰⁻¹⁷ It is a good way to expand the chemistry of chelidamic acid and master its function or reaction conditions to research a variety of metal complexes with chelidamic acid.

The aim of this work is to report and extend the contribution on chelidamic acid chelating with other metal ions based on the syntheses, structures and properties of its cobalt(II), nickel(II) derivatives.

Experimental Section

Materials and Physical Measurements. All reagents and solvents were purchased from commercial sources and used without further purification. The IR spectra were recorded on a Nicolet Magna 750 FT-IR spectrometer with KBr pellets in the range 4000-400 cm^{-1} . Elemental analyses (C, H, and N) were carried out on a Vario EL III elemental analyzer. TG analyses were performed on a Perkin-Elmer TGA7 instrument with a heating rate of 15 Kmin^{-1} . The magnetic susceptibility data were obtained using a Quantum Design PPMS6000 magnetometer. All data were corrected by the Pascal constants.²¹

Synthesis of Complex 1 ($\text{Ni}(\text{C}_7\text{H}_2\text{NO}_5)_3\text{H}_2\text{O}\cdot\text{H}_2\text{O}\cdot 0.25\text{MeCN}$). A mixture of 73 mg $\text{Ni}(\text{CH}_3\text{COO})_2\cdot 4\text{H}_2\text{O}$, 50 mg H_3Chel and 28 mg KSCN was dissolved in the 20 mL mixture solution of water and acetonitrile in a volume ratio

of 1 : 1. After dropping 1-2 drops of KOH (1 mol/L), the resulting solution was refluxed with constant stirring for 2 hours. The solution was allowed to stand at room temperature. Green crystals of **1** were obtained over a period of 4 days. Elemental analysis (%), Found (calcd): C, 28.15 (28.05); H, 3.28 (3.37); N, 5.52 (5.45). IR (KBr, cm^{-1}), 3245 (vs), 2729 (m), 2617 (m), 2515 (m), 1605 (vs), 1466 (w), 1416 (s), 1389 (vs), 1331 (m), 1263 (m), 1057 (s), 939 (w), 872 (m), 808 (s), 744 (m), 702 (w), 580 (w), 521 (w), 444 (w).

Synthesis of Complex 2 ($\text{Co}(\text{C}_7\text{H}_2\text{NO}_5)_3\text{H}_2\text{O}\cdot\text{H}_2\text{O}\cdot 0.25\text{MeCN}$). **2** was synthesized with 62 mg $\text{Co}(\text{CH}_3\text{COO})_2\cdot 2\text{H}_2\text{O}$ in a similar way as for **1**. Deep red crystals of **2** were obtained over a period of 3 days. Elemental analysis (%), Found (calcd): C, 28.10 (28.03); H, 3.32 (3.37); N, 5.49 (5.45). IR (KBr, cm^{-1}), 3246 (vs), 2725 (m), 2617 (m), 2511 (m), 1603 (vs), 1464 (w), 1417 (s), 1387 (vs), 1336 (m), 1261 (m), 1049 (s), 941 (w), 872 (m), 806 (s), 744 (m), 703 (w), 579 (w), 513 (w), 444 (w).

X-ray Crystallography. Table 1 provides the summary of the crystal data, data collection, and refinement parameters for **1** and **2**. Diffraction data were collected on a Rigaku Mercury CCD diffractometer for the present compounds with graphite-monochromatic Mo $K\alpha$ radiation ($\lambda = 0.71073$ Å) by the ω scan mode at 293 K. Empirical correction of absorption was applied for the two complexes. Both structures were solved by direct methods and refined anisotropically by full-matrix least squares based on F^2 for all the non-hydrogen atoms. For both of the compounds, the hydrogen atoms were placed in calculated positions with assigned isotropic thermal parameters, $U(\text{H}) = 1.2U_{\text{eq}}(\text{C})$, and allowed to ride on their parent atoms. Computations were carried out using the SHELXTL PC program system.¹⁸

Crystallographic data for the structures reported here have been deposited with CCDC (Deposition No.: CCDC-234644 for complex **1** and 234645 for complex **2**). These data can be obtained free of charge via <http://www.ccdc.cam.ac.uk/>

Table 1. Crystallographic Data For **1** and **2**

	1	2
Empirical formula	C ₇ H ₁₀ N ₃ O ₅ Ni	C ₇ H ₁₀ N ₃ O ₅ Co
Color and Habit	Green platelet	Deep red prism
Crystal Size (mm)	0.30 × 0.20 × 0.10	0.66 × 0.40 × 0.38
Crystal system	Monoclinic	Monoclinic
Space group	C2/c	C2/c
a (Å)	14.625(6)	14.658(6)
b (Å)	6.996(3)	7.078(3)
c (Å)	22.446(9)	22.681(2)
β (°)	91.397(4)	91.59(5)
V (Å ³)	2295.8(2)	2352.2(1)
Z	8	8
Mr	321.13	321.35
D _c (Mg/m ³)	1.858	1.815
μ (mm ⁻¹)	1.735	1.503
F(000)	1316	1308
θ range (°)	3.23 to 25.03	3.20 to 25.03
Limiting indices	-16 ≤ h ≤ 17, -8 ≤ k ≤ 7, -26 ≤ l ≤ 26	-17 ≤ h ≤ 17, -8 ≤ k ≤ 8, -26 ≤ l ≤ 26
Reflections measured	6978	6493
Independent reflections	2026 (R _{int} = 0.0275)	2013 (R _{int} = 0.0556)
Absorption correction	Sphere (Rigaku CrystalClear)	Sphere (Rigaku CrystalClear)
Relative Transmission Factor	0.8522-1.0000	0.5697-1.0000
Parameter/Restraints/Data (obs.)	177 / 1 / 1828	177 / 1 / 1959
Goodness-of-fit	1.000	1.004
Final R indices (obs.)	R1 = 0.0503, wR2 = 0.1498	R1 = 0.0690, wR2 = 0.1953
R indices (all)	R1 = 0.0556, wR2 = 0.1562	R1 = 0.0724, wR2 = 0.1970
Largest difference peak (e-Å ⁻³)	1.170, -0.730	0.914, -0.816

$$R1 = (\sum |F_o - |F_c||) / \sum |F_o|, wR2 = [\sum w((F_o^2 - F_c^2)^2) / \sum w |F_o|^2]^{1/2}$$

conts/retrieving.html or from CCDC, 12 Union Road, Cambridge CB2 1EZ, UK, email: deposit@ccdc.cam.ac.uk.

Results and Discussion

Description of the Structures.

Triaqua(4hydroxypyridine-2,6dicarboxylato-k³N,O,O')-M(II)acetonitrile-water(1/0.25/1): The selected bond distances and angles for [M(C₇H₂NO₅)(H₂O)₃].0.25 (C₂H₃N)(H₂O) (M = Ni(II) **1**, Co(II) **2**) are listed in Table 2. The drawing of the molecular structure is shown in Figure 1.

The two compounds presented are isostructures with the same space group C2/c, and compound **1** is discussed in details. The coordination environment of the metal atoms in **1** and **2** is six-coordinated by one nitrogen and two oxygen atoms from the chelidamic acid ligand and three water molecules to form a distorted octahedral conformation, as shown in Figure 1. The center atoms and the Chelidamic acid ligand in **1** and **2** are coplanar with a mean deviation of 0.019(2) Å and 0.024(2) Å, respectively. The three Ni-O(water) bond distances are not equal, in which those with the coordinated water molecules occupying the axial positions of octahedron (Ni-O1W = 2.087(4) Å and Ni-O2W = 2.083(4) Å) are obviously longer than that with the coordinated water molecule locating on the equatorial plane (Ni-O3W = 2.021(3) Å). The bond angles of nickel(II) ion

Table 2. Selected bond lengths (Å) and angles (°) for **1** and **2**

Ni(1)-N(1)	1.964(4)	Co(1)-N(1)	2.036(2)
Ni(1)-O(1W)	2.087(4)	Co(1)-O(1W)	2.140(3)
Ni(1)-O(2W)	2.083(4)	Co(1)-O(2W)	2.132(2)
Ni(1)-O(3W)	2.021(3)	Co(1)-O(3W)	2.035(2)
Ni(1)-O(11)	2.192(3)	Co(1)-O(11)	2.214(2)
Ni(1)-O(13)	2.117(3)	Co(1)-O(13)	2.163(2)
O(15)-C(13)	1.338(6)	O(15)-C(13)	1.351(3)
N(1)-Ni(1)-O(1W)	93.1(2)	N(1)-Co(1)-O(1W)	93.0(1)
N(1)-Ni(1)-O(2W)	95.3(2)	N(1)-Co(1)-O(2W)	95.8(2)
N(1)-Ni(1)-O(3W)	174.7(1)	N(1)-Co(1)-O(3W)	172.6(1)
N(1)-Ni(1)-O(11)	76.7(1)	N(1)-Co(1)-O(11)	75.2(1)
N(1)-Ni(1)-O(13)	78.6(1)	N(1)-Co(1)-O(13)	76.3(1)
O(1W)-Ni(1)-O(2W)	170.8(2)	O(1W)-Co(1)-O(2W)	170.3(2)
O(1W)-Ni(1)-O(3W)	85.4(2)	O(1W)-Co(1)-O(3W)	85.4(2)
O(2W)-Ni(1)-O(3W)	86.6(2)	O(2W)-Co(1)-O(3W)	86.4(2)
O(1W)-Ni(1)-O(11)	89.8(1)	O(1W)-Co(1)-O(11)	89.7(2)
O(2W)-Ni(1)-O(11)	88.7(1)	O(2W)-Co(1)-O(11)	88.5(1)
O(3W)-Ni(1)-O(11)	108.3(1)	O(3W)-Co(1)-O(11)	112.0(2)
O(1W)-Ni(1)-O(13)	92.2(2)	O(1W)-Co(1)-O(13)	92.9(1)
O(2W)-Ni(1)-O(13)	93.0(2)	O(2W)-Co(1)-O(13)	93.2(2)
O(3W)-Ni(1)-O(13)	96.5(1)	O(3W)-Co(1)-O(13)	96.6(2)
O(11)-Ni(1)-O(13)	155.2(1)	O(11)-Co(1)-O(13)	151.5(1)

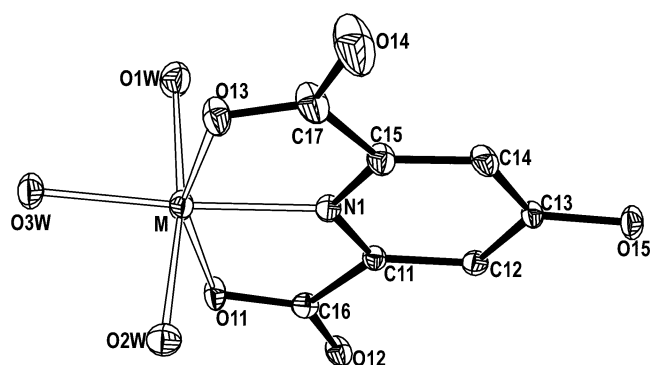


Figure 1. Molecular structure of **1** and **2** showing 30% displacement ellipsoids with H atoms being omitted for clarity.

and neighbor oxygen atoms from water are in the range of $85.4(2)$ – $86.6(2)^\circ$, which are comparable with those of the previously reported zinc analog¹⁷ and iron analog.¹⁶ In contrast, the bond angles of N1–Ni–O11 and N1–Ni–O13 are $78.6(1)$ and $76.7(1)^\circ$, because of the strain of the tridentate ligand. The C13–O15 bond distance in **1** ($1.338(6)$ Å) and **2** ($1.351(3)$ Å), which is close to 1.36 Å characteristic of C–O bonds in aromatic alcohols,¹⁹ indicates that the pyridine ring exhibits the enolic form upon coordination.²⁰ The rest of the N–C, C–C and C–O bond distances of the Chelidamic acid ligand are all agree well with those found in chelidamic acid.⁹

The atoms O3W and O11 of the nickel complex act as hydrogen bond acceptors to form intermolecular hydrogen bonds with the atoms O14 and O15 from another one with the O3W⋯O14 distance of $2.868(6)$ Å and the O11⋯O15 distance of $2.635(4)$ Å, respectively. As shown in Figure 2, the above two types of hydrogen bonds link the nickel complexes to form an infinite chain extending along the $[1\ 1\ 0]$ direction, which interlinks with its crystallographic inversion center-related chain through the O2W⋯O12 hydrogen bonds ($2.834(5)$ Å) to form a double chain. The neighboring double chains are H-bonding bridged by lattice water molecules O4W (O1W⋯O4W = $2.844(6)$, O2W⋯O4W = $2.831(6)$ Å) and interlinked through O1W⋯O12 hydrogen bonds ($2.717(5)$ Å) to form a layer-like structure along the $[0\ 1\ 0]$ direction. The layers are interlinked to each other through the O4W⋯O14 and O3W⋯O13 hydrogen bonds (O4W⋯O14 = $2.714(7)$, O3W⋯O13 = $2.695(5)$ Å) to form a 3-D framework along the $[0\ 0\ 1]$ direction, between

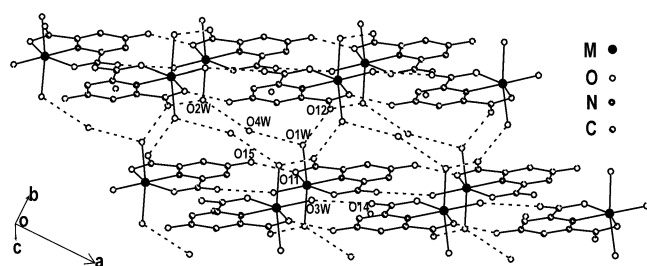


Figure 2. Layer-like structure of the title complexes constructed by hydrogen bonds. Dashed lines represent the hydrogen bonds.

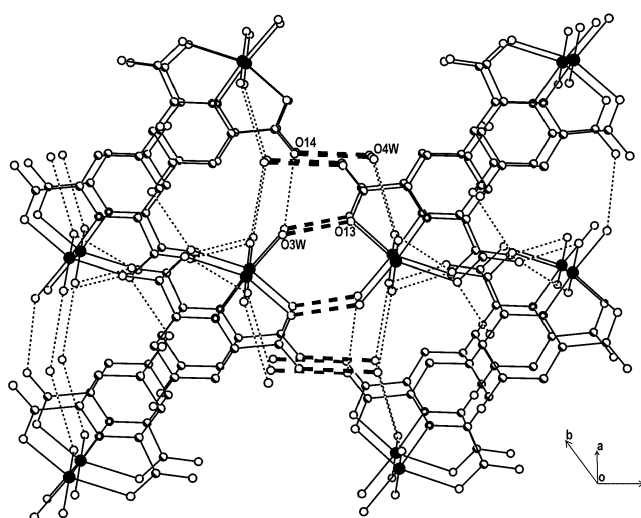


Figure 3. Molecular packing diagram of the title complexes. The interlayer hydrogen bonds are represented as thick dashed lines.

which the disordered acetonitrile molecules are located (the hydrogen bonds around the acetonitrile molecules are not discussed here), as shown in Figure 3.

Unlike the previously reported analogs of V, Cr and Fe, it is worth noting that the bond lengths of M–O11 in **1** and **2** are $0.075(3)$ and $0.051(2)$ Å longer than those of the M–O13, respectively, which is probably due to the existence of a O15⋯O11 hydrogen bond. A similar case is also found in the Zn analog.¹⁷

Chemical Properties: The TG analysis showed that the two complexes were steady as they lost little weight until about 100°C (loss of about 2%). The TG analysis of a pure sample of **1** (6.581 mg) in nitrogen flow showed continuous steps of weight loss (from 37.1 to 263.2°C), which corresponded to the water and acetonitrile loss (exp. 25.06%, calc. for $(\text{H}_2\text{O})_3 \cdot 0.25(\text{C}_2\text{H}_3\text{N}) \cdot (\text{H}_2\text{O})$ 25.62%). Similar to **1**, the TG analysis of a pure sample of **2** (5.255 mg) in nitrogen flow showed continuous steps of weight loss from 26.6 to 249.2°C , which corresponded to the water and acetonitrile loss (exp. 24.99%, calc. for $(\text{H}_2\text{O})_3 \cdot 0.25(\text{C}_2\text{H}_3\text{N}) \cdot (\text{H}_2\text{O})$ 25.64%).

Variable-temperature magnetic susceptibility data were collected for the pure crystal sample of **2**. The temperature-dependent magnetic susceptibility measurement for **2** has confirmed that the cobalt ion is in a formal oxidation state of -2 by which the cobalt compound satisfied the neutrality requirement. A $1/\chi_M - T$ plot in Figure 4 shows that the phase is paramagnetic over 5 – 300 K. For **2** (Co), in the $70 < T < 300$ K range, a non-linear fit via $\chi_M = C/(T - \theta) + \chi_0$ reveals a Curie-Weiss behavior with the Curie constant $C = 2.89(2)$ $\text{cm}^3\text{mol}^{-1}\text{K}$, the Weiss constant $\theta = -16.3(4)$ K, and the background susceptibility, $\chi_0 = 5.4 \times 10^{-4}$ cm^3/mol . The large negative Weiss constant indicates that it is possible for spin-orbit coupling and an antiferromagnetic interaction to exist, which assume to be transferred by the intermolecular hydrogen bonds and the dipole-dipole exchange interaction.

An effective magnetic moment of $4.81 \mu_B$ can thus be

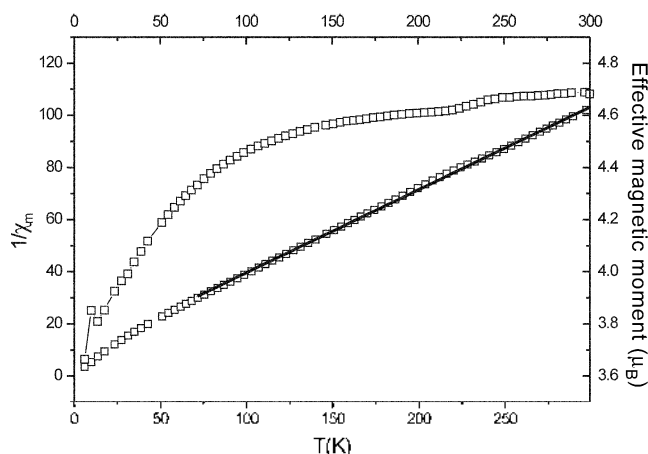


Figure 4. Inverse molar susceptibility with temperature for **2**. The gradual but significant decrease of μ_{eff} upon cooling suggests the presence of antiferromagnetic interactions.

obtained for each Co center, which lies within the range of typical experimental values ($4.3\text{--}5.2 \mu_{\text{B}}$).²¹ It is obviously higher than the spin-only one ($\mu_{\text{eff}} = 3.87 \mu_{\text{B}}$)²¹ suggesting that there is a small orbital angular moment contribution to the effective magnetic moment of the cobalt(II) ion. The antiferromagnetic interaction is reflected in the $\mu_{\text{eff}}\text{--}T$ plot of Figure 4 with the effective magnetic moment decreased upon cooling ($\mu_{\text{eff}} = 2.828 \cdot (\chi_{\text{M}}'T)^{1/2} \mu_{\text{B}}$, $\chi_{\text{M}}' = \chi_{\text{M}} - \chi_{\text{0}}$). The significant decrease of μ_{eff} for **2** at low temperatures is considered to be one result of the zero-field splitting of ground state. However, the origin for the small dip around 10 K for **2** (Co) in Figure 4 is still unclear.

As the crystal structure of **2** showing a distorted octahedral coordination geometry around the cobalt(II) ion, the $S = 3/2$ state splits into two zero-field splitting states because of the axial distortion and the spin-orbit coupling interaction. The spin Hamiltonian (± 1) takes on the form (D is ZFS parameter): $\hat{H} = g\beta\hat{S} \cdot \vec{H} + D[\hat{S}_z^2 - S(S-1)/3]$, from which the energy levels could be figured out. After the substituting of each energy level into the Van Vleck equation, the two following formulas of magnetisability are deduced (in the formulas, $x = D/kT$):

$$\chi_{\parallel} = \frac{Ng^2\beta^2}{4kT} \frac{1 + 9\exp(-2x)}{1 + \exp(-2x)}$$

$$\chi_{\perp} = \frac{Ng^2\beta^2}{4kT} \frac{1 + 3/4x(1 - \exp(-2x))}{1 - \exp(-2x)}$$

From the formula $\chi_{\text{m}} = (\chi_{\parallel} + 2\chi_{\perp})/3$, considering the intermolecular interaction and introducing the molecular field correction,²¹ the following equation applies: $\chi_{\text{m}}' = \chi_{\text{m}} / (1 - 2zJ\chi_{\text{m}}/Ng^2\beta^2)$. Via this equation, an $\chi_{\text{m}}\text{--}T$ plot in Figure 5 shows the fitting of variable-temperature magnetic susceptibility data with $D/k = -6.31$ K, $g = 2.73$, $zJ/k = -2.58$ K. The negative zJ value suggests that an antiferromagnetic interaction exists in **2**, which gives the same conclusion as the result of the fitting via the Curie-Weiss's Law.

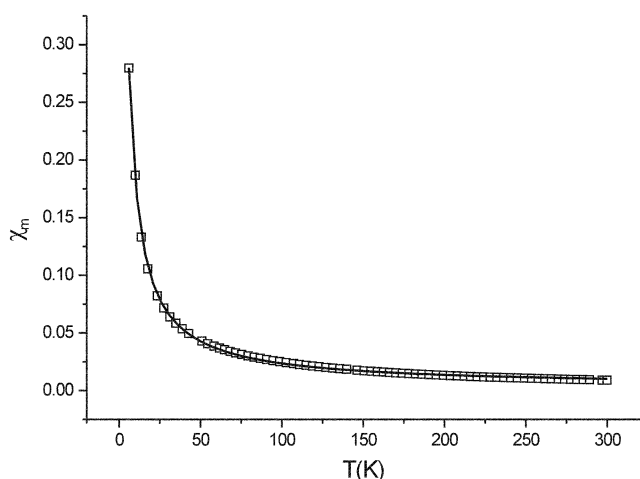


Figure 5. Fitting of the variable-temperature magnetic susceptibility data. (Zero field splitting formula. Molecular field correction in addition)

Table 3. Hydrogen bonds

1		2	
O1W ^{***} O12	2.717(5)	O1W ^{***} O12	2.731(3)
O1W ^{***} O4W	2.844(6)	O1W ^{***} O4W	2.858(4)
O2W ^{***} O12	2.834(5)	O2W ^{***} O12	2.848(3)
O2W ^{***} O4W	2.831(6)	O2W ^{***} O4W	2.839(4)
O3W ^{***} O13	2.695(5)	O3W ^{***} O13	2.691(3)
O3W ^{***} O14	2.868(6)	O3W ^{***} O14	2.814(4)
O4W ^{***} O14	2.714(7)	O4W ^{***} O14	2.749(4)
O11 ^{***} O15	2.635(4)	O11 ^{***} O15	2.653(3)

Acknowledgement. We gratefully acknowledge the financial support of the National Natural Science Foundation of China (20001007, 20131020) and the Natural Sciences Foundation of the Chinese Academy of Sciences (KJXC2-H3) and Fujian Province (20031031).

References

- Berl, V.; Hue, I.; Khoury, R. G.; Lehn, J.-M. *Chem. Eur. J.* **2001**, *7*, 2798-2809.
- Ng, S. W. *J. Organomet. Chem.* **1999**, *585*, 12-17.
- Nakatsujii, Y.; Bradshaw, J. S.; Tse, P.-K.; Arena, G.; Wilson, B. E.; Wilson, N. K.; Dalley, N. K.; Izatt, R. M. *Chem. Commun.* **1985**, 749-751.
- Boger, D. L.; Hong, J.; Hikota, M.; Ishida, M. *J. Am. Chem. Soc.* **1999**, *121*, 2471-2477.
- Fessmann, T.; Kilburn, J. D. *Angew. Chem. Int. Ed. Engl.* **1999**, *38*, 1993-1996.
- Bridger, G. J.; Skerlj, R. T.; Padmanabhan, S.; Martellucci, S. A.; Henson, G. W.; Struyf, S.; Witvrouw, M.; Schols, D.; Clercq, E. De. *J. Med. Chem.* **1999**, *42*(19), 3971-3981.
- Searcey, M.; McClean, S.; Madden, B.; McGown, A. T.; Wakelin, L. P. G. *Anti-Cancer Drug Des.* **1998**, *13*, 837-855.
- Riegel, E. R.; Reinhard, M. C. *J. Am. Chem. Soc.* **1926**, *48*, 1334-1345.
- Bag, S. P.; Fernando, Q.; Freiser, H. *Acta Crystallogr.* **2000**, *C56*, 407-411.
- Ng, S. W. *Z. Kristallogr.* **1998**, *213*, 421-426.

11. Ng, S. W. *J. Organomet. Chem.* **1999**, *585*, 12-17.
 12. Riegel, R. *J. Am. Chem. Soc.* **1926**, *48*, 1334-1345.
 13. Hall, A. K.; Harrowfield, J. M.; Skelton, B. W.; White, A. H. *Acta Crystallogr., Sect. C (Cr. Str. Comm.)* **2000**, *56*, 448-450.
 14. Cline, S. J.; Skallesoe, Pedersen, E.; Hodgson, D. J. *Inorg. Chem.* **1979**, *18*, 796-801.
 15. Yang, L.; Cour, A. L.; Anderson, O. P.; Crans, D. C. *Inorg. Chem.* **2002**, *24*, 6322-6331.
 16. Thich, J. A.; Ou, C. C.; Powers, D.; Vasiliou, B.; Mastropaolo, D.; Potenza, J. A.; Schugar, H. J. *J. Am. Chem. Soc.* **1976**, *98*, 1425-1433.
 17. Zhou, G.-W.; Guo, G.-C.; Liu, B.; Wang, M.-S.; Guo, G.-H.; Cai, L.-Z.; Huang, J.-S. *Acta Crystallogr., Sect. E* **2003**, *59*, m926-m928.
 18. *SHELXTL Version 5.0*; Siemens Industrial Automation Inc., Analytical Instrumentation; Madison, WI, 1995.
 19. Sutton, L. E. *Chem. Soc., Special Publ.* **1965**, *18*, S16s-S21s.
 20. Gaspar, A. B.; Muñoz, C. M.; Niel, V.; Real, J. A. *Inorg. Chem.* **2001**, *40*, 9-10.
 21. Carlin, R. L. *Magnetochemistry*; Springer-Verlag: Berlin, 1986.
-